Bull. Astr. Soc. India (2003) **31**, 19–36

Optical observations of the bright long duration peculiar GRB 021004 afterglow

S.B. Pandey[1], D.K. Sahu[2,3], L. Resmi[4,5], R. Sagar[1,3], G.C. Anupama[3], D. Bhattacharya[4], V. Mohan[1], T.P. Prabhu[3], B.C. Bhatt[2,3], J.C. Pandey[1], Padmaker Parihar[2,3] and A.J. Castro-Tirado[6]

[1] *State Observatory, Manora Peak, Nainital – 263 129, India*
[2] *Center for Research & Education in Science & Technology, Hosakote, Bangalore – 562 114, India*
[3] *Indian Institute of Astrophysics, Bangalore – 560 034, India*
[4] *Raman Research Institute, Bangalore – 560 080, India*
[5] *Joint Astronomy Programme, Indian Institute of Science, Bangalore – 560 012, India*
[6] *Instituto de Astrofísica de Andalucía, P.O. Box 03004, E-18080, Granada, Spain*

Received 6 November 2002; accepted 10 February 2003

Abstract. The CCD magnitudes in Johnson B,V and Cousins R and I photometric passbands are determined for the bright long duration GRB 021004 afterglow from 2002 October 4 to 16 starting $\sim$ 3 hours after the $\gamma-$ray burst. Light curves of the afterglow emission in B,V,R and I passbands are obtained by combining these measurements with other published data. The earliest optical emission appears to originate in a revese shock. Flux decay of the afterglow shows a very uncommon variation relative to other well-observed GRBs. Rapid light variations, especially during early times ($\Delta t < 2$ days) is superposed on an underlying broken power law decay typical of a jetted afterglow. The flux decay constants at early and late times derived from least square fits to the light curve are 0.99 ± 0.05 and 2.0 ± 0.2 respectively, with a jet break at around 7 day. Comparison with a standard fireball model indicates a total extinction of $E(B-V) = 0.20$ mag in the direction of the burst. Our low-resolution spectra corrected for this extinction provide a spectral slope $\beta = 0.6 \pm 0.02$. This value and the flux decay constants agree well with the electron energy index $p \sim 2.27$ used in the model. The derived jet opening angle of about 7° implies a total emitted gamma-ray energy $E_\gamma = 3.5 \times 10^{50}$ erg at a cosmological distance of about 20 Gpc. Multiwavelength observations indicate association of this GRB with a star forming region, supporting the case for collapsar origin of long duration GRBs.

Keywords : Photometry – spectroscopy – GRB afterglow – flux decay – spectral index

1. Introduction

In recent years, both photometric and spectroscopic optical observations of Gamma-Ray Burst (GRB) afterglows have provided valuable information about the emission from GRBs. While spectral lines have been used to determine redshift distances and to study the host galaxies, photometric light curves have unravelled the physical parameters and dynamical evolution of GRB afterglows (cf. Panaitescu & Kumar 2002, Sagar 2001, 2002 and references therein).

A long duration GRB 021004 ($\equiv$ H2380) triggered at $12^h06^m13.^s57$ UT on 4 October 2002 was detected by the HETE FREGATE, WXM, and soft $X-$ray camera (SXC) instruments (Shirasaki et al. 2002). The burst had a duration of $\sim$ 100 seconds in both FREGATE 8-40 Kev and WXM 2-25 Kev bands. Analyses of the FREGATE and WXM data by Lamb et al. (2002) show that the spectrum of the burst is well characterized by a single power-law with slope 1.64$\pm$0.09. The burst fluences are 0.75, 1.8 and 3.2 μerg/cm^2 in the energy bands of 2 – 25 Kev, 50 – 300 Kev and 7 – 400 Kev respectively. The fluence ratio S(2-25)/S(50-300) = 0.42 indicates that it is an $X-$ray rich GRB.

The SXC coordinates of the burst reported by Doty et al. (2002) are $\alpha = 00^h26^m55.^s75, \delta = +18°56'18.''6$ (J2000). A relatively bright with $R \sim 15.5$ mag optical afterglow (OA) of the GRB 021004 was discovered by Fox (2002) about 9 minutes after the burst at $\alpha = 00^h26^m54.^s687, \delta = +18°55'41.''3$ (J2000) with an uncertainty of $0.''5$ in each coordinates. The astrometric position of the OA determined by Henden & Levine (2002) is $\alpha = 00^h26^m54.^s674, \delta = +18°55'41.''59$ (J2000) with $\sim$ 50 mas external error in each coordinates. This is in excellent agreement with the coordinates given by Fox (2002). Thus, GRB 021004 becomes second burst after GRB 990123 whose OA could be observed within few minutes of the trigger of the event. At the location of OA, Wood-Vasey et al. (2002) found no source brighter than $R \sim 22$ mag on images taken on 3 October 2002 at $07^h24^m18^s, 07^h54^m50^s$ and $08^h25^m19^s$ UT while Sako & Harrison (2002) report a fading $X-$ray source with a power-law time slope of -1.1 ± 0.1 using the Chandra $X-$ray observations taken with the High-Energy Transmission Grating on 2002 October 5, about 20.5 hours after the burst. Almost within a day after the burst, the radio afterglow was also detected by Frail & Berger (2002) at 22.5 GHz; by Pooley (2002) at 15 GHz and by Bremer & Castro-Tirado (2002) at 86 GHz. The polarimetric observations taken on 2002 October 05.077 and 08.225 UT indicate almost zero $V-$band intrinsic polarization for the OT (Covino et al. 2002; Rol et al. 2002, Wang et al. 2002).

Based on the detection of ionised Mg, Mn and Fe absorption features, Fox et al. (2002) indicated two redshift values, z = 1.38 and 1.60. Eracleous et al. (2002) and Anupama et al. (2002) also confirm the presence of two absorption systems. Chornock & Filippenko (2002) identified in addition to them, the emission lines at z = 2.323. The existence of this multi-component z $\sim$ 2.3 redshift systems was also confirmed by Castro-Tirado et al. (2002), Djorgovski et al. (2002), Mirabal et al. (2002b), Salamanca et al. (2002) and Savaglio et al. (2002) in the high resolution spectrum of the OA. The spectroscopic variability studied by Matheson et al. (2003) indicates that there is a colour evolution with the OA becoming redder with time, implying a (B-V) increase of about 0.2 - 0.3 mag over the first three days. The spectrum of the OA consists of a blue

continuum with several absorption features corresponding to two intervening metal-line systems at $z = 1.380$ and 1.602 and one set of lines at a redshift of z = 2.323, apparently intrinsic to the host galaxy of the GRB. Møller et al. (2002), on the other hand, identify absorption lines from five systems at z = 1.3806, 1.6039, 2.2983, 2.3230 and 2.3292 along with an emission line at z = 2.3351.

There are no photometric standards in the field of GRB 021004 and the photometric calibrations published after the burst by Weidinger et al. (2002) and Henden (2002) show a zero-point difference of 0.12 mag in *R*. A comparison of Henden (2002) photometry with that of Barsukova et al. (2002) for 3 common star indicates that former is brighter by 0.2 to 0.3 mag in *B*; fainter by 0.01 to 0.11 mag in *V* but agrees within errors in *R*. For reliable determination of the OA magnitudes, secured photometric calibrations are needed. In order to provide them, we imaged the field of GRB 021004 along with SA 92 standard region of Landolt (1992). A total of 40 secondary stars in the field have been calibrated and their standard *BVRI* magnitudes are given here. Our observations started about 3 hour after the burst and are valuable for dense temporal coverage of the light curve. We present the details of our optical observations in the next section, and discuss the optical light curves and other results in the remaining sections.

2. Optical observations, data reductions and calibrations

The broad band photometric and low-resolution spectroscopic optical observations obtained for the GRB 021004 afterglow are described below along with their data reduction and calibration.

2.1 Broad band photometric data

The broad band Johnson *BV* and Cousins *RI* observations of the OA were carried out between 4 to 16 October 2002 using 2-m Himalayan Chandra Telescope (HCT) of the Indian Astronomical Observatory (IAO), Hanle and the 104-cm Sampurnanand telescope of the State Observatory, Nainital. At Nainital, one pixel of the 2048 × 2048 pixel^2 size CCD chip corresponds to $0.''38$ square, and the entire chip covers a field of $\sim 13' \times 13'$ on the sky. The gain and read out noise of the CCD camera are 10 e^-/ADU and 5.3 e^- respectively. At Hanle, one pixel corresponds to $0.''3$ square, and the entire chip covers a field of $\sim 10' \times 10'$ on the sky, it has a read out noise of 4.95 e^- and gain is 1.23 e^-/ADU. From Nainital, the CCD *BVRI* observations of the OA field along with Landolt (1992) standard SA 92 region were obtained on 13/14 October 2002 during good photometric sky conditions for photometric calibration. During the observing run, several twilight flat field and bias frames were also obtained for the CCD calibrations.

The CCD frames were cleaned using standard procedures. Image processing was done using ESO MIDAS, NOAO IRAF and DAOPHOT softwares. Atmospheric extinction coefficients determined from the Nainital observations of SA 92 bright stars are 0.34, 0.22, 0.17 and 0.14 mag in B, V, R and I filters respectively on the night of 13/14 October 2002. They are used in our further analyses. There are nine standard stars in the SA 92 region. They cover a wide range in

colour ($0.64 < (V-I) < 1.84$) as well as in brightness ($12.5 < V < 15.6$). The transformation coefficients were determined by fitting least square linear regressions to the following equations.

$b_{CCD} = B - (0.036 \pm 0.01)(B-V) + (5.08 \pm 0.02)$
$v_{CCD} = V - (0.051 \pm 0.01)(B-V) + (4.56 \pm 0.01)$
$r_{CCD} = R - (0.003 \pm 0.01)(V-R) + (4.38 \pm 0.01)$
$i_{CCD} = I - (0.026 \pm 0.01)(V-R) + (4.87 \pm 0.02)$

where $BVRI$ are standard magnitudes and $v_{CCD}, b_{CCD}, r_{CCD}$ and i_{CCD} represent the instrumental magnitudes normalized for 1 second of exposure time and corrected for atmospheric extinction. The errors in the colour coefficients and zero points are obtained from the deviation of data points from the linear relation. Using these transformations, $BVRI$ photometric magnitudes of 40 secondary standard stars are determined in the GRB 021004 field and their average values are listed in Table 1. The (X,Y) CCD pixel coordinates are converted into $\alpha_{2000}, \delta_{2000}$ values using the astrometric positions given by Henden (2002). All these stars have been observed 3 to 17 times in a filter and have internal photometric accuracy better than 0.01 mag. Henden (2002) also provides the $UBVRI$ photometry for a large number of stars in the field. A comparison in the sense present minus Henden (2002) value yields small systematic zero-point differences of $-0.002 \pm 0.03, 0.013 \pm 0.02, 0.02 \pm 0.026$ and 0.03 ± 0.03 mag in B, V, R and I filters respectively. These numbers are based on 25 common stars having range in brightness from $V = 14$ to 18 mag and can be accounted for in terms of zero-point errors in the two photometries. There is no colour dependence in the photometric differences. We therefore conclude that photometric calibration used in this work is secure.

Several short exposures up to a maximum of 15 minutes were generally given while imaging the OA (see Table 2). In order to improve the signal-to-noise ratio of the OA, the data have been binned in 2×2 pixel^2 and also several bias corrected and flat-fielded CCD images of OA field taken on a night are co-added in the same filter, when found necessary. From these images, profile-fitting magnitudes are determined using DAOPHOT software. For determining the difference between aperture and profile fitting magnitudes, we constructed an aperture growth curve of the well isolated stars and used them to determine aperture (about 5 arcsec) for the magnitudes of the OA. They are calibrated differentially with respect to the secondary standards listed in Table 1 and the values derived in this way are given in Table 2. They supersede the values published earlier by Sahu et al. (2002).

The secondary standards are also used for calibrating other photometric measurements of OA published by the time of paper submission by Bersier et al. (2003), Covino et al. (2002), Di Paola et al. (2002), Fox (2002), Garnavich & Quinn (2002), Holland et al. (2003), Halpern et al. (2002a, b), Malesani et al. (2002a, b), Masetti et al. (2002), Matsumoto et al. (2002), Mirabal et al. (2002a, b), Oksanen et al. (2002), Rhoads et al. (2002), Stefanon et al. (2002), Williams et al. (2002), Winn et al. (2002) and Zharikov et al. (2002). In order to avoid errors arising due to different photometric calibrations, we have used only those published $BVRI$ photometric measurements whose magnitudes could be determined relative to the stars given in Table 1. The JHK magnitudes are adopted from Di Paola et al. (2002), Rhoads et al. (2002) and Stefanon et al. (2002). The distribution of photometric data points taken from the literature and from the

Table 1. The identification number(ID), (α,δ) for epoch 2000, standard $V,(B-V),(V-R)$ and $(R-I)$ photometric magnitudes of the stars in the GRB 021004 region are given. N(B,V,R,I) denotes the number of observations taken in B,V,R and I filters respectively. Star 23 is the comparison star mentioned by Henden (2002).

ID	α_{2000} (h m s)	δ_{2000} (deg m s)	V (mag)	$B-V$ (mag)	$V-R$ (mag)	$V-I$ (mag)	N(B,V,R,I)
1	00 26 29	18 54 28	17.287	0.750	0.428	0.765	(9,9,17,9)
2	00 26 31	18 55 20	14.412	0.876	0.487	0.873	(9,10,16,10)
3	00 26 32	18 55 56	17.321	0.813	0.467	0.908	(9,10,17,9)
4	00 26 32	18 57 09	15.708	1.097	0.637	1.151	(9,10,17,9)
5	00 26 34	18 54 43	16.924	0.642	0.379	0.703	(9,10,17,9)
6	00 26 34	18 57 00	17.701	0.703	0.383	0.746	(9,10,17,10)
7	00 26 35	18 51 49	15.743	1.043	0.621	1.090	(9,10,17,9)
8	00 26 37	18 54 51	14.399	0.653	0.373	0.706	(9,10,16,10)
9	00 26 38	18 58 19	14.704	0.787	0.423	0.802	(9,10,16,10)
10	00 26 39	18 56 01	13.234	1.072	0.557	1.044	(9,9,7,3)
11	00 26 44	18 51 56	14.199	0.669	0.372	0.683	(9,10,16,10)
12	00 26 46	18 55 24	13.906	0.717	0.385	0.767	(9,10,16,10)
13	00 26 48	18 56 33	16.746	0.900	0.504	1.016	(9,10,17,10)
14	00 26 51	18 54 37	17.514	0.606	0.340	0.694	(9,10,17,10)
15	00 26 51	18 59 10	17.469	1.481	1.111	2.426	(9,10,17,10)
16	00 26 51	18 57 47	17.862	0.760	0.429	0.887	(9,10,17,10)
17	00 26 52	18 55 12	14.449	1.072	0.609	1.111	(9,10,17,9)
18	00 26 53	19 02 23	15.646	0.885	0.506	0.942	(9,10,17,10)
19	00 26 54	18 52 24	16.125	0.740	0.413	0.774	(9,9,17,9)
20	00 26 54	18 53 45	17.985	0.580	0.349	0.668	(8,9,15,9)
21	00 26 58	18 56 08	16.717	0.617	0.355	0.725	(9,10,17,10)
22	00 26 58	18 59 51	11.670	0.640	0.386	0.758	(3,4,3,3)
23	00 26 59	18 56 57	16.273	1.149	0.711	1.360	(9,10,17,10)
24	00 27 01	18 51 16	15.680	1.075	0.638	1.142	(9,10,17,10)
25	00 27 01	18 54 16	17.325	0.484	0.309	0.666	(9,10,17,9)
26	00 27 05	18 55 50	15.352	0.618	0.359	0.726	(9,10,17,10)
27	00 27 05	18 55 51	17.356	0.652	0.394	0.810	(9,10,17,10)
28	00 27 06	18 58 18	16.139	0.626	0.366	0.744	(9,10,17,10)
29	00 27 06	19 03 10	17.506	1.054	0.652	1.174	(7,7,11,5)
30	00 27 07	18 52 21	17.958	0.662	0.349	0.735	(9,9,17,10)
31	00 27 08	18 57 08	17.118	0.777	0.449	0.878	(9,10,17,10)
32	00 27 08	18 59 36	13.580	0.912	0.510	0.961	(9,10,16,10)
33	00 27 09	19 01 59	16.041	1.151	0.690	1.226	(9,10,17,10)
34	00 27 10	19 00 48	17.769	1.463	0.994	2.024	(9,10,17,10)
35	00 27 12	18 55 39	16.722	1.139	0.716	1.297	(9,10,17,10)
36	00 27 13	18 51 35	17.476	0.842	0.496	0.946	(9,9,17,10)
37	00 27 13	18 54 08	16.125	0.914	0.573	1.068	(9,10,17,10)
38	00 27 13	19 02 45	17.420	1.427	0.916	1.686	(8,9,15,9)
39	00 27 14	18 56 24	16.096	0.832	0.480	0.938	(9,8,14,9)
40	00 27 15	18 59 12	15.252	1.055	0.610	1.145	(5,6,14,8)

present measurements are $N(U,B,V,R,I,J,H,K) = (6,25,31,197,23,2,3,3)$ and $N(B,V,R,I) = (15,27,67,29)$ respectively. Thus, a total of 428 photometric data points in eight passbands are there for our analysis in the optical and near-IR region.

2.2 Spectroscopic observations

CCD low-resolution spectra of the OA were obtained, from IAO, on 2002 October 4.789, 4.806, 4.876 and 4.894 UT, using the Hanle Faint Object Spectrograph Camera instrument. The epochs

Table 2. CCD BVRI broad band optical photometric observations of the GRB 021004 afterglow. At Hanle, 2-m HCT was used while at Nainital, 104-cm Sampurnanand optical telescope was used.

Date (UT) of 2002 October	Magnitude (mag)	Exposure time (Seconds)	Telescope	Date (UT) of 2002 October	Magnitude (mag)	Exposure time (Seconds)	Telescope
	B– passband				*V*– passband (continued)		
04.725000	18.37±0.01	600	104-cm	07.878831	20.80±0.02	3×600 + 400	HCT
04.728681	18.43±0.01	600	HCT	08.818565	21.20±0.03	2×600	HCT
04.733333	18.43±0.01	600	104-cm	08.856076	21.21±0.03	2×600	HCT
04.741667	18.52±0.01	600	104-cm	10.778611	21.77±0.04	3×600	HCT
04.833333	18.87±0.01	600	104-cm	10.828819	21.66±0.03	3×600	HCT
04.834109	18.88±0.02	600	HCT	10.881933	21.71±0.04	3×600	HCT
04.841667	18.95±0.01	600	104-cm	11.851632	21.91±0.03	4×600	HCT
04.850000	18.96±0.01	600	104-cm		*I*– passband		
04.928472	19.19±0.02	300	104-cm	04.671528	16.48±0.01	300	104-cm
04.929329	19.21±0.02	600	HCT	04.679861	16.56±0.01	300	104-cm
04.960544	19.31±0.02	600	HCT	04.684722	16.58±0.01	300	104-cm
04.982639	19.33±0.02	300	104-cm	04.745602	17.20±0.01	300	HCT
05.673588	20.33±0.02	1200	HCT	04.768750	17.31±0.01	300	104-cm
05.809676	20.53±0.02	1200	HCT	04.773611	17.36±0.01	300	104-cm
05.871713	20.62±0.02	1200	HCT	04.778472	17.32±0.01	300	104-cm
	V– passband			04.850660	17.54±0.01	300	HCT
04.691667	17.53±0.01	600	104-cm	04.861806	17.48±0.02	100	104-cm
04.700000	17.64±0.01	600	104-cm	04.936806	17.68±0.04	50	104-cm
04.713889	17.70±0.01	600	104-cm	04.938032	17.77±0.02	300	HCT
04.737870	17.99±0.02	400	HCT	04.976389	17.84±0.06	50	104-cm
04.784722	18.29±0.01	600	104-cm	05.646030	18.83±0.02	600	HCT
04.792361	18.31±0.01	500	104-cm	05.712882	18.86±0.01	600	HCT
04.800000	18.33±0.01	500	104-cm	05.834213	19.11±0.02	600	HCT
04.843495	18.45±0.02	400	HCT	05.895949	19.19±0.02	600	HCT
04.856250	18.45±0.01	200	104-cm	06.756343	19.51±0.02	600 + 300	HCT
04.932640	18.70±0.01	100	104-cm	06.775690	19.48±0.02	600 + 300	HCT
04.944792	18.73±0.02	400	HCT	06.893345	19.62±0.03	2×500	HCT
04.965278	18.83±0.01	100	104-cm	07.908241	20.05±0.05	4×250 + 300	HCT
04.969132	18.84±0.02	400	HCT	07.927083	19.85±0.11	6×300	104-cm
05.658657	19.81±0.02	900	HCT	08.675694	20.31±0.07	6×300	104-cm
05.680671	19.86±0.01	3×900	104-cm	08.869317	20.35±0.05	400 + 300	HCT
05.725729	19.89±0.02	600	HCT	08.884282	20.35±0.04	3×300	HCT
05.823009	20.02±0.02	600	HCT	08.903009	20.45±0.05	3×300	HCT
05.886007	20.13±0.03	600	HCT	09.829167	20.46±0.10	2×900	104-cm
06.730463	20.48±0.02	2×600	HCT	10.809030	21.00±0.14	2×900	104-cm
06.864549	20.54±0.02	3×600	HCT	11.760470	21.30±0.14	4×300	104-cm
				14.750690	21.64±0.18	3×900	104-cm

correspond to 0.285, 0.302, 0.372 and 0.39 day respectively after the burst. The exposure times were 900s for the first two and 1200s for the last two spectra. They were obtained at a resolution of 18 Å, using a slit width of 2″, covering a wavelength range of 5200–9000 Å. Spectrophotometric standard BD+28° 4211 was observed with a wider slit of 15″ width.

All spectra were bias subtracted, flat-field corrected, extracted and wavelength calibrated in the standard manner using the IRAF reduction package. The spectra were corrected for instrumental response and brought to a flux scale using the spectrophotometric standard. Since the position angle of the slit was not along the parallactic angle (Filippenko 1982), and the observations were made at an airmass ~ 2.2, the fluxes of the OA have been calibrated using zero points derived from *BVRI* photometry. The spectra have been corrected for a total (Galactic and/or host galaxy) extinction of $E(B-V) = 0.20$ mag (see section 4 for details) and shown in Fig 1. The

Table 2. (Continued)

Date (UT) of 2002 October	Magnitude (mag)	Exposure time (Seconds)	Telescope	Date (UT) of 2002 October	Magnitude (mag)	Exposure time (Seconds)	Telescope
	R– passband				*R*– passband (continued)		
04.625694	16.74±0.01	300	104-cm	05.886806	19.73±0.02	3×900	104-cm
04.631944	16.73±0.01	300	104-cm	05.908704	19.70±0.02	900	HCT
04.637500	16.75±0.01	300	104-cm	05.952072	19.72±0.02	900	HCT
04.642361	16.81±0.01	300	104-cm	06.648611	20.04±0.02	4×900	104-cm
04.654861	16.87±0.01	300	104-cm	06.700972	19.98±0.02	3×600	HCT
04.684051	17.06±0.01	60	HCT	06.807998	20.08±0.02	3×600	HCT
04.690694	17.12±0.01	300	HCT	06.835880	20.09±0.01	3×600	HCT
04.697257	17.22±0.01	300	HCT	06.926921	20.15±0.02	3×600	HCT
04.703125	17.27±0.01	300	HCT	07.820856	20.38±0.02	4×400	HCT
04.709213	17.28±0.02	300	HCT	07.887847	20.37±0.02	2×400 + 500	HCT
04.715000	17.31±0.02	300	HCT	07.898611	20.50±0.09	5×300	104-cm
04.720972	17.41±0.02	300	HCT	07.948611	20.43±0.13	3×300	104-cm
04.749306	17.73±0.01	300	104-cm	08.645139	20.69±0.04	6×300	104-cm
04.753438	17.76±0.02	300	HCT	08.769491	20.71±0.03	600 + 500	HCT
04.754167	17.74±0.01	300	104-cm	08.793299	20.72±0.03	2×600	HCT
04.759028	17.77±0.01	300	104-cm	09.727234	20.96±0.03	3×500	HCT
04.763194	17.81±0.01	300	104-cm	09.766319	20.99±0.02	3×600	HCT
04.825417	17.93±0.01	300	HCT	09.800000	21.12±0.06	3×900	104-cm
04.856667	18.07±0.01	300	HCT	09.810069	20.95±0.02	4×600	HCT
04.859028	18.06±0.02	100	104-cm	10.706250	21.29±0.06	2×900	104-cm
04.920810	18.29±0.02	300	HCT	10.711505	21.23±0.03	2×500	HCT
04.934722	18.35±0.04	50	104-cm	10.732951	21.22±0.03	400 + 300	HCT
04.940278	18.31±0.02	300	104-cm	11.722220	21.55±0.11	2×900 + 2×300	104-cm
04.945139	18.38±0.02	300	104-cm	11.799398	21.44±0.03	3×500	HCT
04.954167	18.37±0.02	300	104-cm	11.846667	21.43±0.03	3×500	HCT
04.967361	18.48±0.03	50	104-cm	13.675613	21.91±0.05	5×500	HCT
05.616771	19.28±0.02	900	HCT	13.716991	21.93±0.05	6×400	HCT
05.633576	19.34±0.02	900	HCT	13.756940	21.71±0.08	2×900	104-cm
05.641667	19.42±0.02	4×600	104-cm	14.659720	21.87±0.11	2×900 + 1800	104-cm
05.703252	19.42±0.01	600	HCT	14.773877	22.04±0.07	5×500	HCT
05.736042	19.46±0.02	600	HCT	14.815926	22.09±0.06	6×500	HCT
05.785718	19.51±0.01	300	HCT	15.847570	22.22±0.07	4×600	HCT
05.793356	19.55±0.01	600	HCT	15.852780	22.48±0.52	1×1800	104-cm
05.846794	19.59±0.01	600	HCT	16.688738	22.46±0.15	10×600	HCT
05.855926	19.62±0.02	600	HCT				

spectrum shows a blue continuum with superposed absorption features. The absorption systems are identified with two intervening metal-line systems at z = 1.38 and 1.60. The line center of the absorption features, their identification and the inferred redshift values are listed in Table 3. The line systems are marked in Fig 1. Present results supercede the analysis presented by Anupama et al. (2002) and agree well with other spectroscopic determinations published in the literature.

A single power law $F_\nu \propto \nu^{-\beta}$ was found to fit continuum of the observed spectra. A chi-squared minimization for the power law yields an index of $\beta = 0.59 \pm 0.02$ for the averaged, $E(B-V) = 0.20$ mag extinction corrected spectrum. This value becomes 1.07±0.06, if the spectra is corrected only for the Galactic extinction with $E(B-V) = 0.06$ mag which then agrees fairly well with the value of $\beta = 0.96 \pm 0.03$ derived by Matheson et al. (2003).

Table 3. Absorption lines in GRB 021004 afterglow spectrum.

Identification	λ in (Å)		Redshift
	Observed	Rest	
Fe II	5577.8	2343.5	1.380
Fe II	5649.3	2373.7	1.380
Fe II	5669.2	2382.0	1.380
Fe II	6185.0	2599.0	1.379
Fe II	6194.6	2382.0	1.601
Mg II	6655.3	2795.5	1.381
Mg II	6672.7	2802.7	1.381
Fe II	6733.1	2585.9	1.604
Fe II	6762.7	2599.4	1.602
Mg II	7273.1	2795.5	1.602
Mg II	7292.9	2802.7	1.602

3. Optical photometric light curves

We have used the present measurements in combination with the published data to study the flux decay of GRB 021004 afterglow. Fig. 2 shows the plot of photometric measurements as a function of time. The X-axis is log ($\Delta t = t - t_0$) where t is the time of observation and $t_0 = 2002$ October 4.504325 UT is the burst epoch. All times are measured in unit of day.

3.1 Rapid variability in the *BVRI* optical light curve

The flux decay of most of the earlier GRB afterglows is generally well characterized by a single power law $F(t) \propto (t - t_0)^{-\alpha}$, where $F(t)$ is the flux of the afterglow at time t and α is the decay constant. However, optical light curves of GRB 021004 (Fig. 2) show rapid variations with an overall flux decay especially during $\Delta t < 2$ day. Among equally well monitored GRB OA, GRB 021004 appears therefore peculiar. In order to see whether variability is correlated in B, V, R and I passbands or not, we derived photometric colours using optical and near-IR data and list them in Table 4. Where necessary, measurements were interpolated between adjacent data points at one wavelength in order to determine a contemporaneous value with another wavelength. There is no evidence for statistically significant large variation in the photometric colours on these time scales. This result is therefore contrary to the variability of spectroscopic colour reported by Matheson et al. (2003).

In order to ensure that observed variability in the OA is not due to errors in photometric measurements, we also plotted in Fig. 2, the R value of Henden's (2002) comparison star against time which showed no variability while Fig. 2 clearly indicates peculiar behaviour of the light curve showing achromatic variability in *BVRI* passbands during early phase. A large fraction of these observations have been carried out using the 1-m class optical telescopes. This indicates

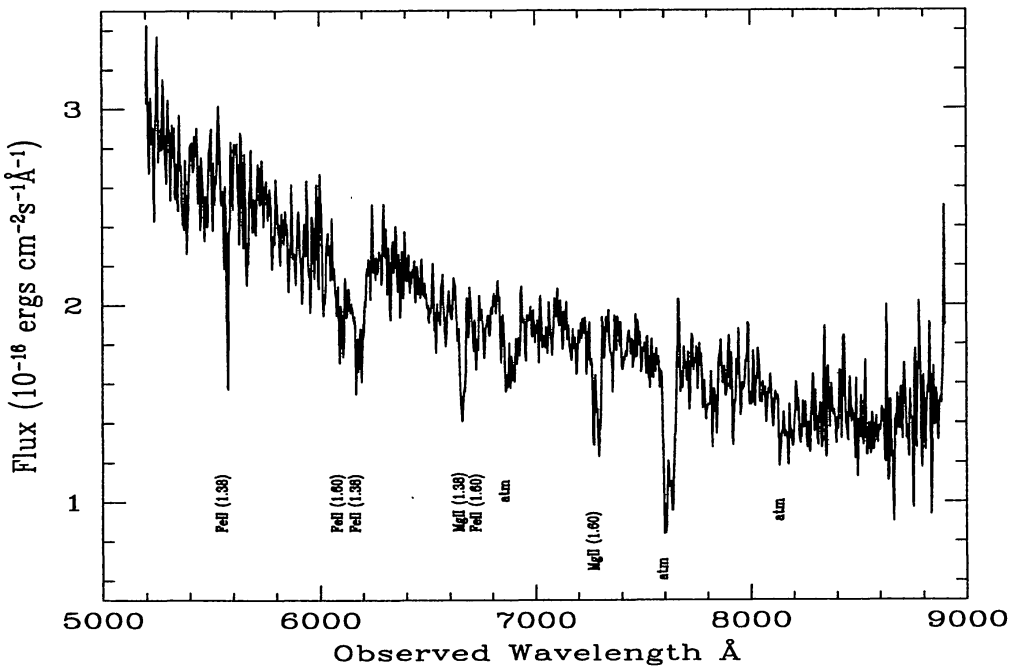

Figure 1. Optical spectrum of the GRB 0021004 OA corrected for $E(B-V) = 0.20$ mag in the wavelength range 5500–9000 Å. The absorption lines are marked along with the estimated redshift value.

that in future large amount of observing time is available on these telescopes (cf. Sagar 2000), will play an important role in understanding the origin of such short term variability in the light curves of GRBs during early times.

In order to analyse the rapid flux variations, we plot in the bottom panel of Fig. 2, residuals after subtracting the best fitted power law values from the corresponding observed ones against time. The variations appear to be achromatic and are clearly visible due to dense temporal coverage of photometric observations. They have a mean of 0.02±0.12, 0.07±0.15, 0.13±0.18 and 0.05±0.15 mag in *B*,*V*,*R* and *I* filters respectively. We obtain a rough estimate of these time variations by fitting gaussian, which gives the FWHM values to be $\sim$ 11.5 and 21 hour for the bumps between $\Delta t = 0.25$ to 1 day and 1.1 to 2.1 day respectively. These periods are considerably larger than 0.7 hour period found by Holland et al. (2002) and Jakobsson et al. (2003) for GRB 011211. The peculiar nature of the GRB 021004 OA can be explained in terms of variable external density of the medium or variation in energy of the blast wave with time (Nakar, Piran & Granot 2003). Lazzati el al. (2002) have also explained this peculiarity in terms of density enhancements of the surrounding medium.

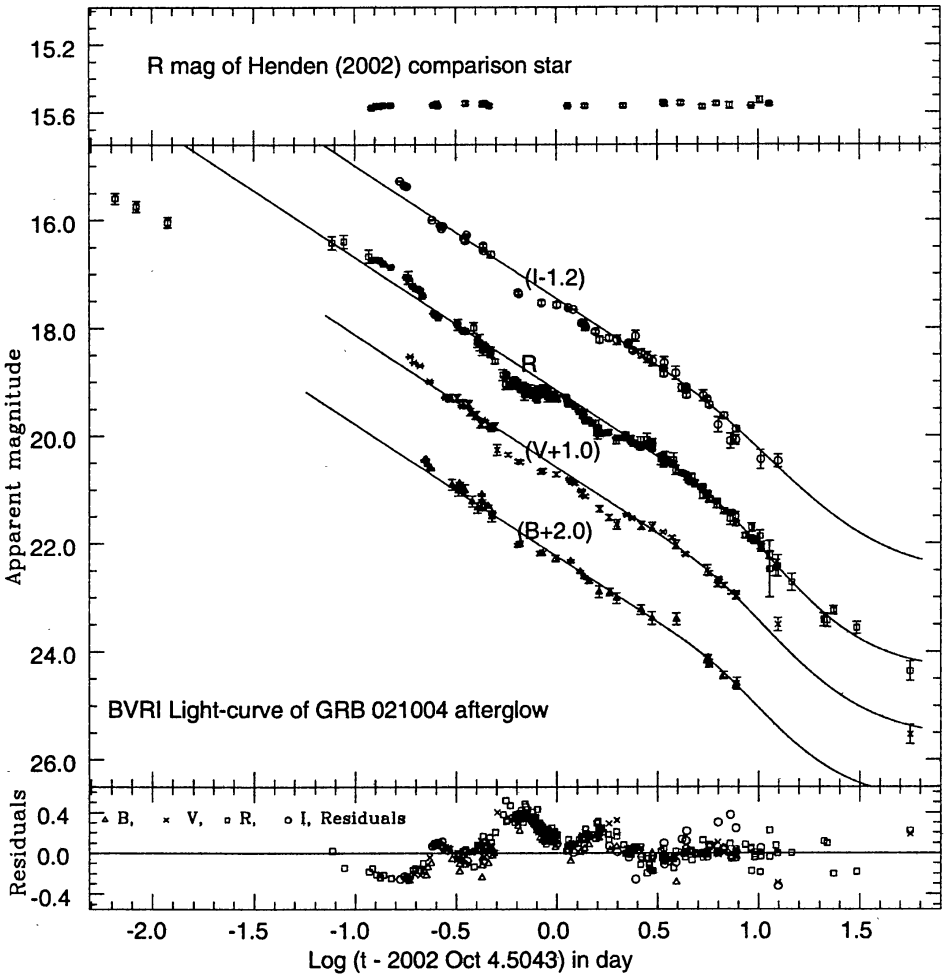

Figure 2. Light curves of GRB 0021004 afterglow in optical photometric *BVRI* passbands are shown in the middle panel. Marked vertical offsets have been applied to avoid overlapping of data points of different passbands. For comparison, R magnitude of Henden (2002) comparison star is also plotted in the upper panel. The *BVRI* band residuals in the sense observed minus power-law fitted magnitudes are displayed in the lower panel.

3.2 Parameters from optical light curves

In the light curves there is steepening after $\Delta t > 6$ day appears to be present in B,V,R and I passbands. Achromatic fluctuations are also clear in *BVRI* passbands. In order to determine the flux decay and related parameters from the optical light curves following analyses have been carried out.

1. The earliest 3 data points in R passband show a flux decay with $\alpha = 0.69 \pm 0.05$. This could

Table 4. Broad band photometric colours of GRB 021004 OA at selected epochs.

Δt (in days)	$(B-V)$ (mag)	$(V-I)$ (mag)	$(B-J)$ (mag)	$(B-H)$ (mag)	$(B-K)$ (mag)
0.22	0.52±0.03				
0.34	0.53±0.03	1.05±0.03			
0.46	0.51±0.03	1.03±0.03			
1.17	0.49±0.03	0.99±0.04			
1.37	0.52±0.04	0.95±0.06	2.2±0.15		4.2±0.3
1.66	0.57±0.05	0.93±0.08	2.3±0.15		3.7±0.3
2.01	0.60±0.06	1.00±0.06		3.3±0.15	
2.98	0.65±0.10	0.98±0.10		3.2±0.15	
5.57	0.63±0.10	1.01±0.10		3.4±0.15	
7.73	0.58±0.10	0.75±0.20			
12.46	0.58±0.10	0.83±0.15			

be due to reverse shock emissions as the value of α is generally around 1.0 during early time flux decay of forward shock emissions (cf. Kobayashi & Zhang 2003 and section 4).

2. It is unlikely that emission from reverse shock will contribute significantly after $\Delta t > 0.1$ day and the steepening in the light curve appears to be 6 days after the burst. We have therefore determined flux decay constant for the OA using least square linear fit to the data points of $\Delta t < 5$ day and found values of 0.92±0.08, 0.93±0.03 and 1.13±0.04 in V,R and I passbands respectively. Average value of the early time flux decay constant of the OA is therefore 0.99±0.05. This is in good agreement with the values of early time flux decay constants of well observed GRB OA and also is as expected theoretically.

3. To determine the late time flux decay constant and break time, we fitted the following empirical function (see Rhoads & Fruchter 2000) which represents a broken power-law in the light curve in presence of underlying host galaxy.

$$m = m_b + \frac{2.5}{s}[log_{10}\{(t/t_b)^{\alpha_1 s} + (t/t_b)^{\alpha_2 s}\} - log_{10}(2)] + m_g$$

where α_1 and α_2 are asymptotic power-law slopes at early and late times with $\alpha_1 < \alpha_2$ and $s > 0$ controls the sharpness of the break, with larger s implying a sharper break. m_b is the magnitude at the cross-over time t_b. m_g is the magnitude of underlying host galaxy. The function describes a light curve falling as $t^{-\alpha_1}$ at $t << t_b$ and $t^{-\alpha_2}$ at $t >> t_b$. In jet models, an achromatic break in the light curve is expected when the jet makes the transition to sideways expansion after the relativistic Lorentz factor drops below the inverse of the opening angle of the initial beam. As there are rapid variations around overall early time flux decay, we fitted the above function in *BVRI* bands, for $\Delta t > 2$ day to determine the parameters of the jet model. In order to avoid a fairly wide range of model parameters for a comparable χ^2 due to degeneracy between $t_b, m_b, m_g, \alpha_1, \alpha_2$ and s, we have used fixed values of $\alpha_1 = 0.99$ and s in our analyses and find that the minimum value of χ^2 is achieved

around $s = 4$. We also fixed the value of m_g for a minimum value of χ^2 for different filters. The fitted values of host galaxy contributions m_g are $\sim$ 24.79, 24.59, 24.35 and 23.79 mag for *B*,*V*,*R* and *I* passbands respectively. The least square fit values of the parameters t_b, m_b, and α_2 are 6.51±0.12 day, 21.37±0.03 mag, and 2.06±0.05 respectively in *R* band, with a corresponding χ^2 of 2.44 per degree of freedom (*DOF*). For *V* passband fitted values of t_b, m_b, and α_2 are 6.44±0.28 day, 21.79±0.06 mag, and 1.96±0.17 respectively with χ^2 3.16 per *DOF*. For *B* and *I* filters we also fixed the value of t_b at 6.5 day to determine the values of α_2. The values of α_2 are 2.07±0.40 and 1.78±0.15 respectively for *B* and *I* filters with m_b values of 22.46±0.03 and 20.87±0.01 mag. For *B* and *I* filters χ^2 values are 1.05 and 2.73 per *DOF*. This indicates that the observed break in the light curve is sharp, unlike the smooth break observed in the optical light curve of GRB 990510 (cf. Stanek et al. 1999; Harrison et al. 1999) but similar to the sharp break observed in the optical light curves of GRB 000301c (cf. Berger et al. 2000, Sagar et al. 2000, Pandey et al. 2001); GRB 000926 (cf. Harrison et al. 2001, Sagar et al. 2001a, Pandey et al. 2001); GRB 010222 (cf. Masetti et al. 2001; Sagar et al. 2001b; Stanek et al. 2001; Cowsik et al. 2001) and GRB 011211 (cf. Jakobsson et al. 2003). In Fig. 2 the best fit light curves obtained in this way for *BVRI* passbands are shown. It can also be seen that our own observations follow the fitted curves very well and fill gaps in the published data.

In the light of above, we conclude that the parameters derived from the optical *BVRI* light curves are $\alpha = 0.69\pm0.05$ for reverse shock emission and $t_b = 6.5\pm0.2$ day, $\alpha_1 = 0.99\pm0.05$ and $\alpha_2 = 2.0\pm0.2$ for the OA. These parameters are improved further in the next section by fitting the multi-wavelength observations with the standard fireball model of GRBs.

4. Modelling of the GRB 021004 afterglow

We attempt modelling the behaviour of GRB 021004 OA along the lines of standard GRB model proposed by Kobayashi & Zhang (2003).

The 7-400 keV gamma-ray fluence (Lamb et al. 2002) implies an isotropic-equivalent energy of 4.6×10^{52} erg emitted in the burst radiation, for $H_0 = 65$ km/s/Mpc in a $\Omega_m = 0.3$, $\Omega_\Lambda = 0.7$ cosmological model. The corresponding comoving passband of $23 - 1330$ keV contains the bulk of the emitted energy in most GRBs, and a k-corrected estimate of Bolometeric energy is unlikely to exceed this by more than $\sim$ 50% (Bloom et al 2001). Assuming a similar amount of energy to remain in the fireball to power the afterglow (Piran et al. 2001), one finds that for a typical $\varepsilon_e \sim 0.1$ and $\varepsilon_B \sim 10^{-2}$ (Panaitescu & Kumar 2001) the frequency ν_m of maximum radiation in the afterglow spectrum should lie close to the optical band at ~ 0.1 day after the burst (Sari, Piran & Narayan 1998; Kobayashi & Zhang 2003). The brightening of GRB 021004 OA optical lightcurve at ~ 0.1 day, relative to the extrapolated early decay, could therefore be attributed to the passage of ν_m through the optical band. The three early *R*-band observations (Fox 2002) which show a power-law decay of $\alpha = 0.69\pm0.05$ before the brightening can then be understood in terms of a decaying prompt emission from the reverse shock (Kobayashi & Zhang 2003). We

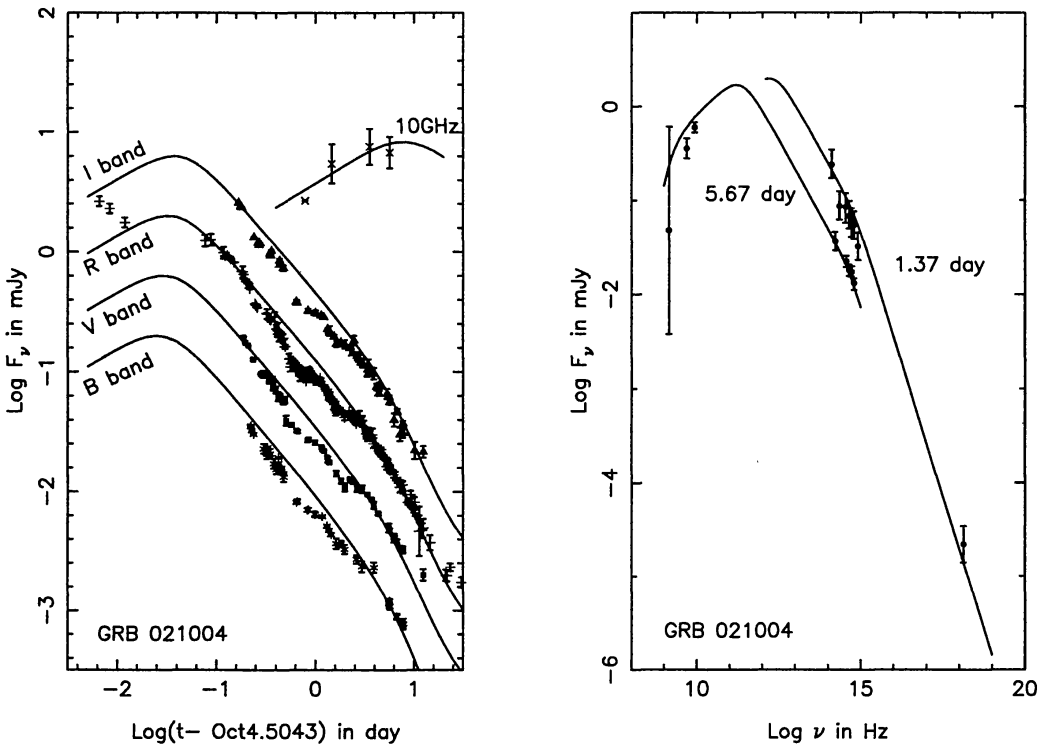

Figure 3. Multi-band observed light curves (left panel) and broadband spectrum (right panel) of the GRB 021004 OA are compared with model predictions shown as solid curves. A total extinction of $E(B-V)$=0.20 mag has been used. For clarity of display, in the left panel the B,V,I and radio light curves are shifted vertically by $-1.0, -0.5, +0.5$ and $+1.0$ respectively in logarithmic scale. The radio light curve at 10 GHz is constructed, by extrapolation with expected spectral slope, from measurements reported at 22.5 GHz, 15 GHz and 8.46 GHz at different epochs (Frail & Berger 2002, Pooley et al. 2002, Berger et al. 2002). The frequency of 10 GHz was chosen to correspond with a similar plot presented by Kobayashi & Zhang (2003). The model uses $\nu_a = 2.1$ GHz, $\nu_m = 2.5 \times 10^{14}$ Hz and $\nu_c = 3.3 \times 10^{16}$ Hz at $t = 0.06$ day; a jet break time $t_b = 6.7$ day and an electron energy distribution index $p = 2.27$. The model includes the host galaxy contribution estimated in section 3.2. In the right panel an expected spectrum with $p = 2.27$ is shown with the Chandra HETG measurement (Sako & Harrison 2002a) and optical and near-IR observations at the same epoch, ~ 1.37 day. A similar spectrum is also shown at $t = 5.67$ day, the epoch of the cm-wave radio observations reported by Berger et al. (2002). Where necessary, fluxes measured at optical, near-IR and radio wavelengths were interpolated between adjacent data points at one wavelength in order to determine a contemporaneous value with another wavelength.

exclude this early emission from our further discussion and restrict ourselves to the properties of the forward shock emission.

In Fig. 3 we compare the predictions of a standard afterglow model with electron energy distribution power-law index p=2.27 and a jet-break time t_b of 6.7 days. For this, the observed mag-

nitudes/fluxes have been corrected for standard Galactic extinction law given by Mathis (1990) and the effective wavelength and normalization by Fukugita et al. (1995) for U,B,V,R,I and by Bessell & Brett (1988) for near-IR have been used. The fluxes thus derived are accurate to about 10% in optical and about 25% in near-IR. For the model parameters mentioned above, relative normalization of the light curves in different optical passbands become consistent with the data if the total extinction is $E(B-V) = 0.20$ mag, which has been used in our analysis. The Galactic extinction in this direction is estimated to be $E(B-V) = 0.06$ mag from the smoothed reddening map provided by Schlegel, Finkbeiner & Davis (1998). The additional extinction may then be attributed to small scale fluctuations in the distribution of dust in our galaxy, or may, in part, originate even in the host galaxy of the GRB. The spectral slope deduced in section 2.2 from the HCT low resolution spectrum is also consistent with $p = 2.27$ once the above total extinction is taken into account. The flux decay constants derived in the last section are also consistent with the parameters used in the model.

Given the above model parameters we find that the broadband behaviour of the OA is well explained. However, such a model cannot reproduce short term variations, as seen during the interval $\sim 0.5-2$ days in the optical light curves (see Fig. 2). The reason for these short term variations could lie in density variations in the circum-burst medium, as conjectured by Lazzati et al. (2002) and Nakar et al. (2003). Fig. 3 shows the broadband spectrum including $X-$ray, optical-near IR and radio observations and the model predictions. The cooling break ν_c is located between the optical and $X-$ray bands. The spectrum observed within the $X-$ray band at $\sim$ 1.37 day (Sako & Harrison 2002a) is $F_\nu \propto \nu^{-1.1\pm0.1}$, and the decay rate is $t^{-1.0\pm0.2}$. Both are consistent with $p = 2.27$ and $\nu > \nu_c$, at a time before the jet break. Our model predictions are also in good agreement with the Chandra observation at $t \sim 52$ day (Sako & Harrison 2002b). The presence of a jet break between the two observations results in the apparent temporal decay slope of ~ 1.7 reported by Sako & Harrison (2002b).

The 1.4 GHz to 8.5 GHz radio spectrum at 5.67 days (Berger et al. 2002) is well fit by the model, assuming a self-absorption frequency ν_a near 2 GHz. The same assumptions lead to a good explanation of the cm-wave radio light curve. Fig. 3 shows the derived light curve at 10 GHz from measurements reported at nearby frequencies (Frail & Berger 2002, Pooley et al. 2002, Berger et al. 2002) and the model prediction. However, this model is unable to reproduce the 85 GHz flux of 2.5 mJy observed at $\Delta t = 1.45$ days (Bremer & Castro-Tirado 2002). Although at the maximum of the spectrum (ν_m) the flux rises to 2.75 mJy in the model, at $\Delta t = 1.45$ days, ν_m is located well above 85 GHz and the predicted flux is only ~ 1 mJy at 85 GHz. It may well be that a part of the emission observed at 85 GHz comes from the host galaxy as in the case of GRB 010222 (Frail et al. 2002) which should be seen to remain visible after the afterglow fades away.

5. Discussions and Conclusions

We present the broad band *BVRI* photometric and low-resolution spectroscopic optical observations of the OA associated with GRB 021004 starting about 3 hour after the burst. Our last

photometric observations are at about Δt = 12 days. These observations in combination with the published multi-wavelength data have been used to study the flux decay and to derive parameters of the GRB and its afterglow. We have used secure photometric calibrations in the present analyses. The optical observations obtained by Fox (2002) during the first 20 minutes of the burst indicate that GRB 021004 is the second GRB OA after GRB 990123 from which optical emission from the reverse shock has been observed (Galama et al. 1999). The dense temporal *BVRI* passband light curve indicates rapid light variations. Such flux variations from a power-law decay have been reported only for GRB 000301c (Sagar et al. 2000a, Masetti et al. 2000, Jensen et al. 2001, Garnavich, Loab & Stanek 2000, Gaudi et al. 2001) and for GRB 011211 (Holland et al. 2002, Jakobsson et al. 2003) so far. However, the amplitude of oscillation is maximum in the case of GRB 021004 OA being $\sim$ 0.5 mag. The light curves show a steepening superposed on the achromatic, rapid variations which could be detected mainly due to the dense observations in *BVRI* filters. This indicates that in future the small telescopes, as large amount of observing time is available on them (cf. Sagar 2000), will play an important role in understanding the origin of such short term variability in the light curves of GRBs during early times. The overall flux decay in observed light curves is well understood in terms of a jet model. The flux decay constants at early and late times derived from least square fits to the light curves are 0.99$\pm$0.05 and 2.0$\pm$0.2 respectively. The value of the jet break time is about 7 day. The total extinction in the direction of the OA is $E(B-V) = 0.2$ mag. The low-resolution spectrum corrected for this extinction yields a spectral slope of $\beta = 0.6\pm0.02$. The photometric colour distributions determined in optical and near-IR regions for various epochs indicate that spectral index of the GRB 021004 afterglow has not changed significantly during a period of about 15 days after the burst, while the flux decay slope has steepened from 1.0 to 2.0. GRB 021004 thus becomes one more burst for which a clear achromatic break in the light curve is observed. This is generally accepted as an evidence for collimation of the relativistic GRB ejecta in accordance with the prediction by recent theoretical models (Mészáros & Rees 1999; Rhoads 1999; Sari Piran & Halpern 1999).

Recent afterglow observations of GRBs show that a relativistic blast wave, in which the highly relativistic electrons radiate via synchrotron mechanism, provides a generally good description of the observed properties. In the case of GRB 021004 OA also, it appears that a standard fireball afterglow model, with a combination of emission from a forward and a reverse shock can account for most of the overall behaviour of the afterglow. The observed fluxes, however, show unexplained fluctuations, falling significantly below model predictions in the range Δt = 0.5–2 days. Density variations in the circum-burst medium is one possible explanation of this behaviour (Wang & Loeb 2000, Lazzati et al. 2002, Nakar et al. 2003, Heyl and Perna 2003). While an alternative explanation in terms of micro-lensing (Garnavich, Loeb & Stanek 2000) cannot be entirely ruled out, the multiple bumps seen in this light curve would not be natural in this model. The observed jet break time of $\sim$ 7 day, along with the burst fluence, leads to an estimate of the jet opening angle of $\sim 7^\circ$ (for an assumed γ–ray efficiency $\eta_\gamma = 0.2$ (Frail et al. 2001), and a circumburst density $n = 0.3$ cm^{-3} inferred from reverse-shock modelling by Kobayashi & Zhang (2003), similar to the opening angles inferred in other jetted afterglows (see, e.g. Panaitescu & Kumar 2001). The inferred opening angle implies a total emitted gamma-ray energy of $E_\gamma \sim 3.5 \times 10^{50}$ erg, close to the peak of the E_γ distribution in GRBs as shown by Frail et al. (2001). The modelling of the radio emission suggests that excess emission might have been

detected at 85 GHz, possibly due to the emission from the host galaxy. If this turns out to be true, then the observed emission would indicate a strong star formation activity in the host galaxy. The multiple blue shifted H, C-IV and Si-IV absorption lines in the spectrum of GRB021004 OA, with a velocity span of 3200 km/s, could be interpreted as a clumpy WC star wind environment (Mirabal et al. 2002b). However our modelling indicates that the light curve after ~ 0.1 day is better explained by a circumburst medium of nearly uniform density with small scale density variations rather than a r^{-2} wind density profile. This might imply a variable mass loss rate in the wind (Heyl and Perna 2003) or that the circumburst medium is composed not of Wolf-Rayet wind but of expanding ejecta of a supernova preceding the burst (Salamanca et al 2002, Wang et al 2003). In either case, these observations provide a strong support in favour of collapsar origin of this burst in particular, and of long duration GRBs in general.

The peculiarity in the light curves of GRB 021004 could be noticed mainly due to dense as well as multi-wavelength observations during early times. Such observations of recent GRBs have started revealing features which require explanation other than generally accepted so far indicating that there may be yet new surprises in GRB afterglows.

Acknowledgements

We thank an anonymous referee for comments which helped us improve the paper. This research has made use of data obtained through the High Energy Astrophysics Science Archive Research Center Online Service, provided by the NASA/Goddard Space Flight Center. L. Resmi is supported by a CSIR research fellowship.

References

Anupama G.C., Sahu D.K., Bhatt B.C., Prabhu T.P., GCN Observational Report No. 1582
Barsukova E.A., Goranskij V.P., Bestin G.M., Plokhotnichenko V.L., Pozanenko A.S., 2002 GCN Observational Report No. 1606
Berger E., Sari R., Frail D. A., et al., 2000, ApJ, 545, 56
Berger E., Frail D. A., Kulkarni S.R., 2002, GCN Observational Report No. 1612, 1613
Bersier D., et al., 2003, ApJL, in press (astro-ph/0211130)
Bessell M.S., Brett J.M., 1988, PASP, 100, 1134
Bloom J.S., Frail D.A., Sari R., 2001, ApJ, 121, 2879
Bremer M., Castro-Tirado A.J., 2002, GCN Observational Report No. 1590
Castro-Tirado A.J., Perez E., Gorasabel J., et al., 2002 GCN Observational Report No. 1635
Chornock R., Filippenko A.V., 2002, GCN Observational Report No. 1605
Covino S., Ghisellini G., Malesani D., et al., 2002, GCN Observational Report Nos. 1595, 1622
Cowsic R., Prabhu T. P., Anupama G. C. et al., 2001, BASI, 29, 157
Di Paola A., Boattini A., Del Principe M., Konstantinova T., Larionor V., Antonelli L., 2002, GCN Observational Report No. 1616
Djorgovski S.G., Barth A., Price P., et al., GCN Observational Report No. 1620
Doty J., Grew G., Jernigan J.G., et al. 2002, GCN Observational Report No. 1568
Eracleous M., Schaeter B.E. Moder J., Wheeler G., 2002, GCN Observational Report No. 1579

Filippenko A.V., 1982, PASP, 94, 715
Fox D.W., 2002, GCN Observational Report No. 1564
Fox D.W., Barth A.J., Soderberg A.M., et al., 2002, GCN Observational Report No. 1569
Frail et al. 2001, ApJ, 562, L55
Frail D.A., Berger E., 2002, GCN Observational Report No. 1574
Frail et al. 2002, ApJ, 565, 829
Fukugita M., Shimasaku K., Ichikawa T., 1995, PASP, 107, 945
Galama T.J. et al., 1999, Nature, 398, 394
Garnavich P.M., Loeb, A.& Stanek K. J., 2000, ApJ, 544, L11
Garnavich P., Quinn J., 2002, GCN Observational Report No. 1661
Gaudi B.S., Granot J., Loeb, A. 2001, ApJ, 561, 178
Halpern J.P., Armstrong E.K., Espaillat C.C., Kemp J., 2002a, GCN Observational Report No. 1578
Halpern J.P. Mirabal N., Armstrong E.K., Espaillat C.C.., Kemp J., 2002b, GCN Observational Report No. 1593
Harrison et al., 1999, ApJ, 523, L121
Harrison F. A., Yost S. A., Sari R. et al., 2001, 559, 123
Henden A., 2002, GCN Observational Report Nos. 1583, 1630
Henden A. & Levine S., 2002, GCN Observational Report No. 1592
Heyl J.S. & Perna R., 2003, ApJL, in press (astro-ph/0211256)
Holland S. T., Soszynski I., Gladders M., et al., 2002, AJ, 124, 639
Holland S. T. et al., 2003, AJ, submitted (astro-ph/0211094)
Jakobsson P., Hjorth J., Fynbo J.U. et al., 2003, submitted to A&A
Jensen B.L., Fynbo J.U., Gorosabel J. et al., 2001, A&A, 370, 909
Kobayashi S., Zhang B., 2003, ApJ, 582, L75
Lamb D., Ricker G., Atteia J-L., et al., GCN Observational Report No. 1600
Landolt, A.R., 1992, AJ, 104, 340
Lazzati D., Rossi E., Covino S., Ghisellino, G., Malcsani D., 2002, A&A, 396, L5
Malesani D., Covino S., Ghisellini G., et al., 2002a, GCN Observational Report No. 1607
Malesani D., Stefanon M., Covino S., et al., 2002b, GCN Observational Report No. 1645
Masetti N. et al., 2001, A&A, 374, 482
Masetti N., Pizzichini G., Bartolini C., et al., 2002, GCN Observational Report No. 1603
Mathis J.S., 1990, ARAA, 28, 37
Matheson T., Garnavich P.M., Foltz G. C., et al., 2003, ApJ, 582, L5
Matsumoto K., Kawabata T., Ayani K., Urata Y., Yamaoka H., Kawai N., 2002, GCN Observational Report No. 1594
Mészáros P., Rees M. J., 1999, MNRAS, 306, L39
Mirabal N., Armstrong E.K., Halpern J.P., Kemp J., 2002a, GCN Observational Report No. 1602
Mirabal N., Halpern J.P., Chornock R., Filippenko A.V., 2002b, GCN Observational Report No. 1618
Møller, P., Fynbo, J.P.U., Hjorth J. et al., 2002, A&A, 396, L21
Nakar, E., Piran,T., Granot,J., 2002, Submitted to New Astronomy (astro-ph/0210631)
Oksanen A., Aho M., Rivich K., Rivich K., West D., Durig D., 2002, GCN Observational Report No. 1591
Panaitescu A., Kumar P., 2001, ApJ, 560, L49
Panaitescu A., Kumar P., 2002, ApJ, 571, 779
Pandey S.B., Sagar R., Mohan V., Pandey A.K, Bhattacharya D., & Castro-Tirado A.J., 2001, BASI, 29, 459
Piran T., Kumar P., Panaitescu A., Piro L. 2001, ApJ, 560, L167
Pooley G., 2002, GCN Observational Report Nos. 1575, 1588, 1604
Rhoads J.E., 1999, ApJ, 525, 737
Rhoads J. E. & Fruchter A., 2001, ApJ, 546, 117

Rhoads J., Burud J., Freuchter A., 2002, GCN Observational Report No. 1601
Rol, E. et al., 2002, GCN Observational Report No. 1596
Sagar R., 2000, Current Science, 78, 1076
Sagar R., 2001, BASI, 29, 215
Sagar R., 2002, BASI, 30, 237
Sagar R., Mohan V., Pandey S.B., Pandey A.K., Stalin C.S., Castro-Tirado A.J., 2000, BASI, 28, 499
Sagar R., Pandey S.B., Mohan V., Bhattacharya D., Castro-Tirado A.J., 2001a, BASI, 29, 1,
Sagar R., Stalin C. S., Bhattacharya D., Pandey S. B., Mohan V., Castro Tirado A. J., Pramesh Rao A., Trushkin S. A., Nizhelskij N. A., Bremer M. and Castro Cerón J. M., 2001b, BASI, 29, 91
Sahu D.K., Bhatt B.C., Anupama G.C., Prabhu T.P., GCN Observational Report No. 1587
Salamanca I., Rol E., Wijers R., Ellison S., Kaper L., Tanvir N., 2002, GCN Observational Report No. 1611
Sako M., Harrison F.A., 2002a, GCN Observational Report No. 1624
Sako M., Harrison F.A., 2002b, GCN Observational Report No. 1716
Sari R., Piran T., Halpern J. P., 1999, ApJ, 519, L17
Sari R., Piran T., Narayan R., 1998, ApJ, 497, L17
Savaglio S., Fiore F., Israel F. et al., 2002, GCN Observational Report No. 1633
Schlegel D.J., Finkbeiner D.P., Davis M., 1998, ApJ, 500, 525
Shirasaki C., Graziani M., Matsuoka M., et al., 2002, GCN Observational Report No. 1565
Stanek K. Z. et al., 1999, ApJ, 522, L39
Stanek K. Z. et al., 2001, ApJ, 563, 592
Stefanon M., Covino S., Malesani D. et al., 2002, GCN Observational Report No. 1623
Wang L., Baade D., Hoeflich P., Wheeler C. J., 2002, GCN Observational Report No. 1672
Wang L., Baade D., Hoeflich P., Wheeler C. J., 2003, Submitted to ApJL (astro-ph/0301266)
Wang X., Loeb A., 2000, ApJ, 535, 788
Weidinger M., Egholm M. P., Fynbo J.P.U., et al., 2002, GCN Observational Report No. 1573
Williams G., Lindsay K., Milne P., 2002, GCN Observational Report No. 1652
Winn J., Bersier D., Stanek K.Z., Gernavich P., Walker A., 2002, GCN Observational Report No. 1576
Wood-Vasey W.M., Aldering G., Lee B.C. et al., GCN Observational Report No. 1572
Zharikov S., Vazquez R., Benitez G., del Rio S., 2002, GCN Observational Report No. 1577